



# Ab initio simulations of silver film adhesion on $\alpha$ -Al<sub>2</sub>O<sub>3</sub> (0 0 0 1) and MgO (1 0 0) surfaces

Yu.F. Zhukovskii<sup>a,b,\*</sup>, M. Alfredsson<sup>c</sup>, K. Hermansson<sup>c</sup>, E. Heifets<sup>d</sup>, E.A. Kotomin<sup>a</sup>

<sup>a</sup> Institute of Solid State Physics, University of Latvia, Kengaraga 8, LV-1063 Riga, Latvia

<sup>b</sup> Chemistry Department, University of Western Ontario, London, Canada N6A 5B7

<sup>c</sup> Inorganic Chemistry, The Ångström Laboratory, Uppsala University, Box 538, S-751 21 Uppsala, Sweden

<sup>d</sup> Department of Chemistry, University of California, CA 95616 Davis, USA

---

## Abstract

The atomic and electronic structure of the Ag/MgO (1 0 0) and Ag/ $\alpha$ -Al<sub>2</sub>O<sub>3</sub>(0 0 0 1) interfaces are calculated by means of the ab initio Hartree–Fock approach combined with a supercell model. The electronic density distribution and the interface binding energy/equilibrium distance for both interfaces are analyzed. For a complete (1:1) surface coverage of the MgO surface the energetically most favorable adsorption position for the Ag atom is above the O atom. For the Ag/ $\alpha$ -Al<sub>2</sub>O<sub>3</sub> interface the preferable adsorption positions for the Ag atom are over centers of either *large equilateral* oxygen triangles (in Al-substituted sites of Al-terminated corundum surface) or *isosceles* oxygen triangles (over O atoms of a first internal oxygen layer) in O-terminated corundum. This interface is less stable than Ag/MgO (1 0 0), due to a large mismatch between lattice constants of Ag (1 1 1) and  $\alpha$ -Al<sub>2</sub>O<sub>3</sub> (0 0 0 1) surfaces as well as the instability of Ag atoms on the Al-terminated corundum surface. © 1998 Elsevier Science B.V. All rights reserved.

PACS: 68.35.-p; 73.20.-r

Keywords: Ag/ $\alpha$ -Al<sub>2</sub>O<sub>3</sub>; Ag/MgO; Interface; Adhesion; Adsorption; Hartree–Fock method; Electron correlation

---

## 1. Introduction

High-resolution electron microscopy measurements give almost atomic resolution of such technologically important metal/oxide interfaces as Ag/ $\alpha$ -Al<sub>2</sub>O<sub>3</sub> [1] and Ag/MgO [2]. For these interfaces a small adhesion energy is usually associated with a large wetting angle. It has been reported that the silver layer growth gives rise to three-di-

mensional islands [1,2]. On the other hand, a recent low-energy-electron diffraction study has depicted a layer-by-layer growth mode for silver deposits on vacuum-cleaved MgO (1 0 0) surfaces, although such an interface is unstable [3]. Probably, these data do not really contradict each other, because various types of surface structure defects might play an active role in the growth mode. Since both oxides have weak interactions with metals they are ideal substrates for the experimental study of the behavior of two-dimensional metal layers.

---

\* Corresponding author.

Theoretical studies of the adhesion properties of noble metals on insulating oxide substrates are rather scarce. Most of previous theoretical studies of metal adhesion on  $\alpha$ -Al<sub>2</sub>O<sub>3</sub> and MgO surfaces were performed using *Local Density Approximation*, as implemented in a full-potential linearized muffin-tin orbital method (FP LMTO) [4,5]. To go beyond this approximation in studying these systems, we have recently performed exact non-local treatment of the exchange interaction between atoms [6,7]. This is possible due to improvements of the ab initio Hartree–Fock (HF) approach realized in the computer code *Crystal* for periodic systems [8], which now incorporates electron correlation corrections (HF-CC method) [9]. This formalism is found to be well suited for the quantitative analysis of the bonding in the interfacial Ag/Oxide region and is used in the present paper. In this paper, we present the first comparative HF study of Ag/oxide interfaces.

## 2. Theoretical background

The method used in this study is the exact-exchange, periodic HF formalism combined with the electron-correlation corrections calculated using the density-functional theory (DFT) [9]. This later is necessary due to a typical underestimate of the binding energies and overestimate of the bond lengths of molecules with the standard HF approximation. In the framework of HF-CC method, we used mainly Perdew–Wang a posteriori corrections [10]. The basis set for MgO, optimized elsewhere [11], consists of all-electron 8-61G and 8-15G functions (s and sp shells) for Mg and O atoms, respectively. Analogously, for the Al and O atoms of corundum we used the optimized 8-511G/8-411G all-electron basis set (s and sp shells) [12]. To reduce computational efforts, we employed the small-core Hay–Wadt pseudo-potentials for Ag atoms [13], thus reducing the total number of electrons per atom down to 19 ( $4s^2 4p^6 4d^{10} 5s^1$ ). The initial guess for the basis set of bulk silver (311-31G for sp and d shells) was taken from AgCl calculations [14], then the outer exponents were reoptimized [6,7].

### 2.1. The Ag/MgO (1 0 0) interface model

Since the *Crystal* code allows the construction of two-dimensional periodic systems in the form of slabs, we have simulated the Ag/MgO (1 0 0) interface by one or three silver layers atop three layers of oxide substrate for a complete (1:1) surface coverage by metal. Its schematic view is shown in Fig. 1. The optimized value of the lattice constant for the three-layer MgO slab (4.21 Å) is very close to the experimental bulk value (4.205 Å [11]). Neglecting a small mismatch of the lattice constants of fcc Ag and MgO crystals, the ratio of which is about 97%, we fixed the above-mentioned value for a lattice constant along the surface plane, varying only the interfacial (silver–oxide) distance as well as distances between different silver planes. This procedure was performed for all preferential sites of Ag atom adsorption: above the surface Mg and O atoms, and the gaps (Fig. 1.) To improve our previous results for the Ag/MgO interface [6], we used special atomic orbitals for the Ag slabs, centered in hollow sites *D* (Fig. 1); their basis set 1(sp)-1(d)G have been preliminary optimized for the bulk [7].

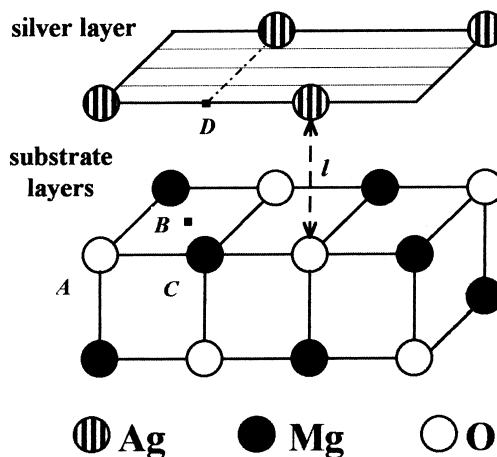


Fig. 1. Fragment of the Ag/MgO (1 0 0) interfacial model where silver atoms are positioned at the distance  $l$  above O atoms of the substrate surface (marked as A configuration). Other two simulated positions are above the gap (B) and Mg atoms (C). Pseudofunctions for the Ag slab are centered on its hollow sites (D).

## 2.2. The $\text{Ag}/\alpha\text{-Al}_2\text{O}_3(0001)$ interface model

For the simulation of a corundum substrate we used a nine-layer slab terminated by Al atoms as shown in Fig. 2. The slab belongs to the hexagonal plane group  $P_{321}$  with a primitive unit cell containing 15 atoms [13]. All the atoms of the O planes are equivalent and form a periodic network of *small* and *large equilateral* triangles with sides  $b_1$  and  $b_2$ , respectively, as well as equal *isosceles* triangles positioned between them. The unit square of each oxygen plane is a rhombus with a side  $a = 4.760$  Å, equal to the length of the translational vector. In bulk corundum all neighbouring O planes are equivalent and separated by  $c = 2.166$  Å. They can be transformed between each other by a syn-

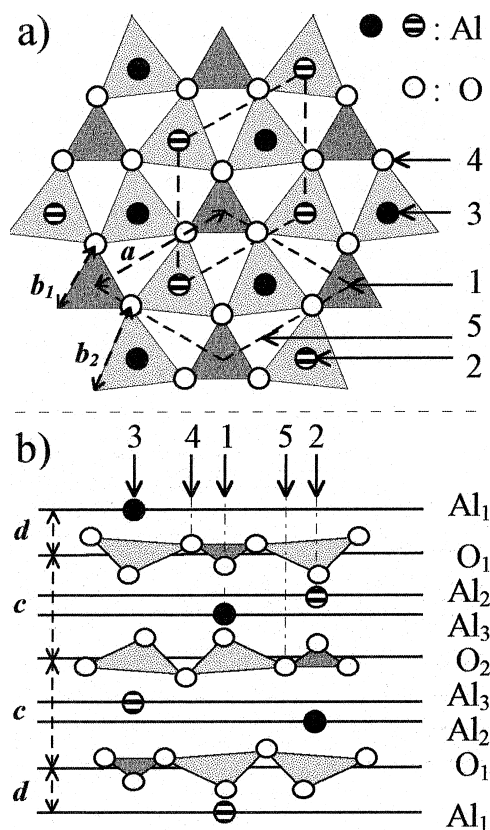


Fig. 2. Top (a) and side (b) views of  $\alpha\text{-Al}_2\text{O}_3(0001)$  slab with parameters  $a$ ,  $b$ ,  $c$  and  $d$ . Symbols  $\text{Al}_1$ ,  $\text{Al}_2$ ,  $\text{Al}_3$ ,  $\text{O}_1$  and  $\text{O}_2$  denote non-equivalent layers. The numbered arrows indicate probable adsorption sites.

chronous combination of a  $30^\circ$  rotation around the corresponding  $C_{3v}$  axes and a translation by  $a/\sqrt{3}$ , so that the two rhombic unit cells shown in Fig. 2 coincide. Each O plane is associated with two Al planes, so each aluminium atom is situated either above (black circles) or below (striped circles) the centers of the large oxygen triangles at the distance  $d = 0.838$  Å. On the Al-terminated  $(0001)$  surface of perfect corundum the outer Al atoms relax towards  $\text{O}_1$  plane. To reduce computational efforts and exploit maximally the system's symmetry, we have simulated an equivalent silver monolayer adsorption on *both* surfaces of the corundum slab. We fixed the substrate structure, except for the interlayer distances  $d$  shown in Fig. 2, and varied the geometry of the Ag layer, including their distances from the substrate and relative positions shown by arrows in Fig. 2. When simulating the  $\text{Ag}/\alpha\text{-Al}_2\text{O}_3(0001)$  interface, we have considered also a seven-layer O-terminated corundum slab with the same coverage of substrate as in the case of pure Al-terminated surface. The plane symmetry of the adsorbed silver film corresponds to the Ag  $(111)$  monolayer with an extended interatomic distance (4.76 Å instead 2.88 Å for bulk silver, the ratio is close to  $\sqrt{3}$ ).

## 3. Results of simulations

### 3.1. Silver film adhesion on $\text{MgO}(100)$

The main results of the simulations performed are summarized in Table 1. For both cases (one and three silver layers) the interfacial Ag atoms position atop the surface O atoms is the energetically most favorable, which is in agreement with previous LDA-type calculations [5]. For the A configuration the equilibrium interface distances calculated by various methods are quite close, falling into narrow interval  $l \in 2.5\text{--}2.7$  Å while the adhesion energy increases substantially when passing from one to three silver layers. As follows from Table 1, other interfacial configurations are less preferable.

The inclusion of special atomic orbitals (pseudo-functions) into the hollow positions D of the Ag slab (Fig. 1) slightly strengthens the interface

Table 1  
Optimized parameters of slab models for the Ag/MgO (1 0 0) interface

| Ag atom over | Type of model | Pseudo-function | Distance $l^{(0)}$ , Å | Adhesion $E_{\text{adh}}$ , eV | Charge $e(00)_{\text{Ag}}$ , a.e. | Dipole $d(10)_{\text{Ag}}$ , a.e. | Quadrupole $q(20)_{\text{Ag}}$ , a.e. |
|--------------|---------------|-----------------|------------------------|--------------------------------|-----------------------------------|-----------------------------------|---------------------------------------|
| O            | Single        | None            | 2.64                   | 0.20                           | 0.028                             | 0.130                             | -2.052                                |
|              | Ag layer      | Included        | 2.56                   | 0.26                           | 0.037                             | 0.198                             | -2.232                                |
|              | 3 layers      | Included        | 2.43                   | 0.46                           | 0.053 <sup>a</sup>                | 0.418 <sup>a</sup>                | -1.971 <sup>a</sup>                   |
| A gap        | Single        | None            | 3.00                   | 0.10                           | 0.025                             | -0.038                            | -1.408                                |
|              | Ag layer      | Included        | 2.94                   | 0.15                           | 0.035                             | -0.034                            | -1.597                                |
|              | 3 layer       | Included        | 2.86                   | 0.17                           | 0.050 <sup>a</sup>                | 0.182 <sup>a</sup>                | -0.963 <sup>a</sup>                   |
| Mg           | Single        | None            | 3.24                   | 0.06                           | 0.015                             | -0.065                            | -1.314                                |
|              | Ag layer      | Included        | 3.23                   | 0.06                           | 0.027                             | -0.071                            | -1.288                                |
|              | 3 layer       | Included        | 3.23                   | 0.07                           | 0.042 <sup>a</sup>                | 0.116 <sup>a</sup>                | -0.686 <sup>a</sup>                   |

<sup>a</sup> For the interface silver layer.

binding and brings the metallic film and the oxide substrate closer [7]. As a result, the adhesion energy (per atom) of the silver monolayer coincides with the experimental estimate of 0.26 eV [3]. However, the introduction of pseudo-functions (and thus improvement of basis set for the Ag slab) does not considerably change our previous results [6].

The effective (Mulliken) charge on the silver atoms reveals a negligible charge transfer from a substrate to adlayer (see column  $e(00)$  in Table 1). According to a difference contour map for charge distribution shown in Fig. 3, the MgO substrate enhances the electron density in the hollow sites D of the silver lattice in the A interface configuration (Fig. 1). On the other hand, the population between the two neighbouring Ag atoms ( $\approx 0.1 e$  per atom in the so-called *bridge* position) practically does not depend on the adsorption position. The atomic dipole moments  $d(10)$  are matrix elements of the atomic orbitals with the operator  $z$  (the direction pointing outwards the surface). The quadrupole moment  $q(20)$  corresponds to the operator  $z^2 - x^2/2 - y^2/2$ . The values of  $d(10)$  and  $q(20)$  for the surface Ag atoms (Table 1) exceed by an order of magnitude those for the substrate atoms (not displayed here). This indicates a strong deformation of the Ag atoms after adsorption on the MgO surface.

The electron density map (Fig. 3) and the bond population analysis indicate a reason why Ag adsorption over the  $\text{O}^{2-}$  ions is favourable: the electrostatic interaction of enhanced electron density

concentrated around the *hollow* position of the interfacial Ag layer ( $\approx 0.07 e$  for the 1:1 Ag coverage) with  $\text{Mg}^{2+}$  ion below it (Fig. 1) is attractive. On the other hand, for Ag adsorption over the  $\text{Mg}^{2+}$  ions, we have a repulsive interaction of electron density localized in the D position with  $\text{O}^{2-}$  ion below. As for the change of the adhesion energy in the case of the *three* Ag layers as compared to a Ag monolayer, it may be explained by a more complicated electron density distribution around the interfacial Ag layer for both the A and C interfacial configura-

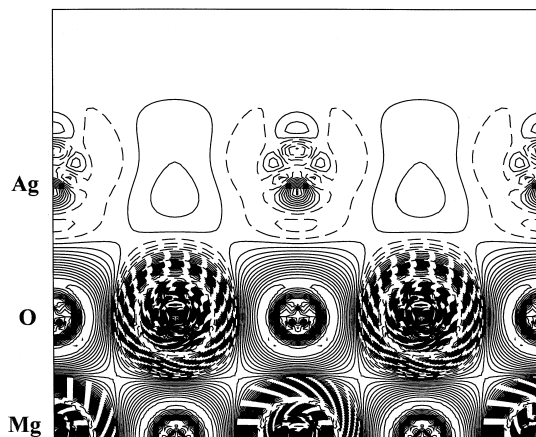


Fig. 3. Difference electron density maps of the silver monolayer adsorbed on the MgO (1 0 0) surface where Ag atoms are placed atop O atoms (Fig. 1) for a cross-section plane perpendicular to the interface and coinciding with (0 0 1) plane passing through A, C, and D points. The full and dashed lines show electron excess and loss, respectively, their increment is  $0.0003 e/\text{a.u.}^3$ .

tions. For the *A* adsorption site,  $\approx 0.04 e$  is localized on the corresponding *hollow* position over  $\text{Mg}^{2+}$ , whereas  $\approx 0.12 e$  is localized on each of the four side *bridge* positions above the D point. For the C adsorption site, the corresponding electron density over  $\text{O}^{2-}$  is smaller ( $\approx 0.03 e$  and  $\approx 0.1 e$ , respectively) and considerably more remote from the surface oxygen ion. A similar explanation may be suggested for the additional increase of the adhesion energy when introducing atomic orbitals in the D positions of both one- and three-layer Ag slabs.

### 3.2. Silver film adhesion on $\text{Al}_2\text{O}_3$ (0 0 0 1)

If Ag atoms are placed on Al-terminated corundum surface (Fig. 2), the SCF procedure does not converge, irrespective of the choice of geometry and computational parameters. This failure is confirmed by earlier studies on metal/corundum interface [4]. Indeed, only very few metals (like  $X = \text{Mg}$ , Ni) interact with Al-top corundum atoms forming a spinel-type surface  $\text{XAl}_2\text{O}_4$ , while the corundum surface exposed to other metals is expected to be O-terminated [15]. Since elementary charge balance arguments make the free O-terminated corundum surface unfavorable, the metal adhesion could in reality take place on steps of (0 0 0 1) terraces as well as other structural defects [1,16]. All the more so because the mentioned mismatch between lattice constants of metal and corundum surfaces can lead to interface reconstruction [17]. To avoid a too complicated structure of the Ag/corundum interface we used the periodic unit cell model of a substrate and *substituted* the Al-top atoms by Ag atoms and then varied their positions with respect to the outer O plane.

The energy minima for the adhesion of a Ag monolayer on the O-terminated corundum surface occur for Ag atoms placed in the Al-substituted 3 sites (above *large equilateral* oxygen triangles) as well as 5 sites (above *isosceles* triangles). But unlike the inward relaxation of the Al-top corundum layer, the Ag atoms here relax outwards, up to 20–25% of the equilibrium distance  $d$  in bulk corundum (Fig. 2). Moreover, the adhesion energy of an Ag monolayer on the O-terminated corundum surface is found to be considerably less compared

with the Al-top layer: 2.8 and 3.0 eV per Ag atom for adsorption sites 3 and 5, respectively, vs. 10.7 eV per Al atom in pure corundum. Usually experimental energies for metal adhesion on corundum are by an order of magnitude smaller than calculated ones because the simulation refers to unstable O-terminated surface [16]. Unlike the case of the Ag/MgO interface, an estimate of the adhesion energy for the Ag/corundum system using the dependence of total energy vs. interfacial distance is complicated by a “polarization catastrophe” (some its examples are described in [8]) as this interfacial distance exceeds by 1.5–1.7 Å the corresponding equilibrium value.

The effective charge transfer towards the oxygen plane differs significantly for pure corundum and the Ag/corundum interface (resulting in net charges of 2.32  $e$  and 0.97  $e$  per Al and Ag atoms in positions 3, respectively). The same is true for the bond populations between metal-top atoms and their nearest O atoms positioned on the  $\text{O}_1$  plane (0.137  $e$  and  $-0.053 e$  for Al–O and Ag–O bonds, respectively). Charge density contour maps shown in Fig. 4 clearly illustrate this difference between the corresponding bond populations. Unlike the Ag/MgO interface there are no areas in the Ag layer with enhanced electron density. At the same

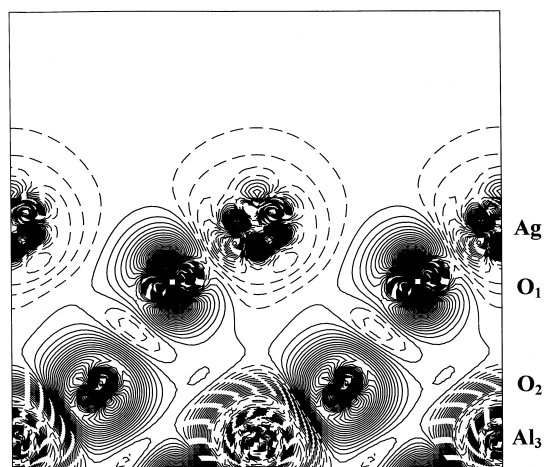


Fig. 4. Difference electron density map of the silver layer adsorbed on the O-terminated corundum (0 0 0 1) surface with Ag placed in the 3 sites (Fig. 2). The plane displayed is perpendicular to the interface and passes through both the Ag–O and Al–O bonds. The same contour levels as in Fig. 3.

time, the analysis of both band structure and DOS shows that, analogously to Ag/MgO system [6], the Ag adhesion on the O-terminated corundum surface occurs because of a significant overlap between Ag 4d and O 2p energy bands of interfacial layers.

#### 4. Conclusions

The general conclusion can be drawn that both the Ag/Al<sub>2</sub>O<sub>3</sub> (0 0 0 1) and Ag/MgO (1 0 0) interfaces formation is a result of physisorption. Moreover, the Ag/Al<sub>2</sub>O<sub>3</sub> (0 0 0 1) interface is unstable because the adhesion of the Ag layer is possible only on the energetically unfavourable O-terminated corundum (0 0 0 1) surface. Introduction of atomic orbitals into the hollow sites of the Ag layers adsorbed on MgO (1 0 0) does not considerably affect our previous results for this interface [6,7], improving them slightly quantitatively. Due to the less dense structure of the Ag layer on the corundum surface, the effect of the substrate interaction with the enhanced electron density in the interatomic positions of the interfacial Ag layer, observed for Ag/MgO (1 0 0) system, is negligible. To simulate the real Ag/Al<sub>2</sub>O<sub>3</sub> and Ag/MgO interfacial structure, it is necessary to incorporate surface defects into consideration and to estimate their effect on preferential adsorption sites and energetics.

#### Acknowledgements

The authors kindly thank the Centers for Computing of both Helsinki University of Technology, Finland, and Aarhus University, Denmark, for provided computer facilities, as well as express their gratitude to M. Causà, V. Kempter, and V.E. Puchin for stimulating discussions.

#### References

- [1] R.M. Pilliar, J. Nutting, *Phil. Mag.* 16 (1967) 181; G.C. Ndubuisi, J. Liu, J.M. Cowley, *Microsc. Res. Tech.* 20 (1992) 439.
- [2] P. Guenard, G. Renaud, B. Vilette, M.-H. Yang, C.P. Flynn, *Scripta Metall. et Mater.* 31 (1994) 1221; A. Trampert, E. Ernst, C.P. Flynn, H.F. Fischmeister, M. Rühle, *Acta Metall. Mater.* 40 (1992) S227.
- [3] F. Didier, J. Jupille, *Surf. Sci.* 307 (1994) 587.
- [4] F.S. Ohuchi, M. Kohyama, *J. Am. Ceram. Soc.* 74 (1991) 1163, review article; C. Kruse, M.W. Finnis, V.Y. Milman, M.C. Payne, A. De Vita, M.J. Gillan, *J. Am. Ceram. Soc.* 77 (1994) 451; C. Kruse, Ph.D. Thesis, Max-Planck-Institut, Stuttgart, 1994.
- [5] U. Schönberger, O.K. Andersen, M. Methfessel, *Acta Metall. Mater.* 40 (1992) S1; T. Hong, J.R. Smith, D.J. Srolovitz, *J. Adhesion Sci. Technol.* 8 (1994) 837.
- [6] E. Heifets, E.A. Kotomin, R. Orlando, *J. Phys.* 8 (1996) 6577; E. Heifets, E.A. Kotomin, *Latv. J. Phys. Techn. Sci.* N5 (1996) 53.
- [7] E. Heifets, Yu.F. Zhukovskii, E.A. Kotomin, M. Causà, *Chem. Phys. Lett.*, in print.
- [8] C. Pisani, R. Dovesi, C. Roetti, *Hartree-Fock Ab Initio Treatment of Crystalline Systems, Lecture Notes in Chemistry*, vol. 48, Springer, Berlin, 1988.
- [9] M. Causà, A. Zupan, *Chem. Phys. Lett.* 220 (1994) 145; R. Dovesi, V.R. Saunders, C. Roetti, M. Causà, N.M. Harrison, R. Orlando, E. Aprà, *CRYSTAL95, User Manual*, University of Turin, Turin, 1996.
- [10] J.P. Perdew, Y. Wang, *Phys. Rev. B* 45 (1991) 13244.
- [11] M. Causà, R. Dovesi, C. Pisani, C. Roetti, *Surf. Sci.* 175 (1986) 551.
- [12] M. Causà, R. Dovesi, C. Pisani, C. Roetti, *Surf. Sci.* 215 (1989) 259; V.E. Puchin, J. Gale, A.L. Shluger, E.A. Kotomin, J. Günster, M. Brause, V. Kempter, *Surf. Sci.* 370 (1996) 190.
- [13] P.J. Hay, W.R. Wadt, *J. Chem. Phys.* 82 (1985) 284.
- [14] E. Aprà, E.V. Stefanovich, R. Dovesi, C. Roetti, *Chem. Phys. Lett.* 186 (1991) 329.
- [15] P. Alemany, R.S. Boorse, J.M. Burlitch, R. Hoffmann, *J. Phys. Chem.* 97 (1993) 8464.
- [16] F. Ernst, *Mater. Sci. Engrg. R* 14 (1995) 97, review article.
- [17] M. Gautier, J.P. Durand, *J. Phys. III (France)* 4 (1994) 1779.